BIOMACROMOLECULES

pubs.acs.org/Biomac Article

Counterpropagating Gradients of Antibacterial and Antifouling Polymer Brushes

Yeongun Ko, Vi Khanh Truong, Sun Young Woo, Michael D. Dickey, Lilian Hsiao, and Jan Genzer*

Cite This: *Biomacromolecules* 2022, 23, 424–430

Read Online

ACCESS | Metrics & More | Article Recommendations | Supporting Information

ABSTRACT: We report on the formation of counterpropagating density gradients in poly([2-dimethylaminoethyl] methacrylate) (PDMAEMA) brushes featuring spatially varying quaternized and betainized units. Starting with PDMAEMA brushes with constant grafting density and degree of polymerization, we first generate a density gradient of quaternized units by directional vapor reaction involving methyl iodide. The unreacted DMAEMA units are then betainized through gaseous-phase betainization with 1,3-propanesultone. The gas reaction of PDMAEMA with 1,3-propanesultone eliminates the formation of byproducts present during the liquid-phase modification. We use the counterpropagating density gradients of quaternized and betainized PDMAEMA brushes in antibacterial and antifouling studies. Completely quaternized and betainized brushes exhibit antibacterial and antifouling behaviors. Samples containing 12% of quaternized and 85% of betainized units act simultaneously as antibacterial and antifouling surfaces.

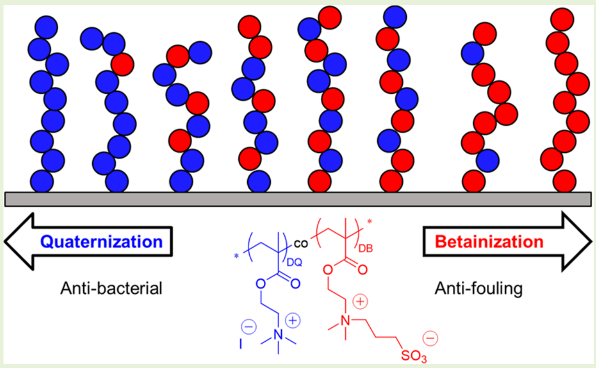

INTRODUCTION

Polymeric coatings have been employed extensively in various applications, including adhesive layers, low friction surfaces, antifouling materials, responsive surfaces, colloidal stabilizers, *etc.*[1−3] Polymers offer higher versatility to tune the physical and chemical properties of surfaces than small-molecule modifiers (*e.g.*, organosilane coupling agents).[4,5] Specifically, surface-grafted polymer assemblies (SGPAs) generate stable coatings on the surface due to chemical covalent bonds.[6,7] To obtain a high grafting density of polymer chains (number of chains per unit area, 1/nm^2), one often uses the "grafting-from" method via surface-initiated atom transfer radical polymerization (SI-ATRP).[7,8] Varying the grafting density, chain length, chain topology, and functional groups of repeat units in SGPA enables fine control of the properties of surfaces.[9,10]

Postpolymerization modification (PPM) is a feasible alternative to a direct polymerization of functional monomers.[11−13] PPM alleviates inherent difficulties found in the direct polymerization of functional monomers.[14] Because PPM does not alter the density and molecular weight of the parent polymers, it allows the direct characterization of a degree of modification and reaction kinetics.[15−17] This point is beneficial for polymer brushes.[18] Under the constant grafting density and degree of polymerization, any changes of physicochemical properties such as dry thickness or a refractive index after PPM modifications can be correlated with the extent of PPM reaction.[16,19] For example, the exposure of poly([2-dimethylaminoethyl] methacrylate) (PDMAEMA) brushes to methyl iodide (MI) results in the rapid formation of quaternized PDMAEMA (qPDMAEMA).[17] Through quaternization, the modified repeat units carry complete positive charges with iodide counterions. The degree of quaternization can be characterized by elemental analysis, Fourier-transform infrared spectroscopy-attenuated total reflection (FTIR-ATR), and ellipsometry.

Another advantage of PPM is that it enables spatial control of the degree of functionality. For instance, a series of charge density gradients in PDMAEMA brushes were generated by the diffusion of MI in the gaseous phase and the reaction within the PDMAEMA brush.[17] Only the charge densities were varied across the sample, while the degree of polymerization and the grafting density remained constant. The gradient width and height could be tuned by changing the concentration of reagent or reaction time. Gradients in chemical or physical properties in films enable the systematic investigation of a particular phenomenon of interest, thereby minimizing experimental error deviations and time-consuming sample preparation while allowing a comprehensive and systematic evaluation of sample attributes.[20−22]

Received: October 24, 2021
Revised: November 30, 2021
Published: December 14, 2021

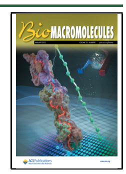

https://doi.org/10.1021/acs.biomac.1c01386
Biomacromolecules 2022, 23, 424−430

Betainization, another modification of the tertiary amines in the PDMAEMA, generates a polyzwitterion containing negative and positive charges in their repeat units.[23] Polyzwitterionic brushes could be formed through either direct polymerization or PPM. In this work, we use PPM to create polyzwitterionic brushes via a gaseous-phase modification of parent PDMAEMA brushes with 1,3-propanesultone (P-S). In solution, P-S can hydrolyze to produce 3-ethoxypropane-1-sulfonic acid, prohibiting betainization by protonating tertiary amines in PDMAEMA.[24] We will discuss that the gaseous-phase modification avoids the generation of the undesired product. We provide details about the reaction kinetics as a function of reaction time and the concentration of P-S.

Charge-bearing polymers play a pivotal role in controlling the interfacial interactions between synthetic and biological species. Specifically, the positively charged PDMAEMA exhibits antibacterial properties against Gram-positive and Gram-negative bacteria.[25] The qPDMAEMA acted similarly to other cationic biocides, attaching directly to bacteria, diffusing through the cell wall, disrupting the cytoplasmic membrane, and killing the bacteria. Polyzwitterions resist nonspecific protein adsorption on surfaces.[26−30] Thus, the polyzwitterionic brushes have often been studied as antifouling surfaces. Here, we developed counterpropagating gradients (CPGs) of quaternized and betainized units in the PDMAEMA brushes through the quaternization gradient followed by betainization of unmodified repeat units. We carry out both PPM reactions in the gaseous phase.[17,31,32] MI and P-S dissolved in ethanol solution are used as quaternization and betainization reagents.[33] We use CPG surfaces to study simultaneously antibacterial and antifouling properties.

■ EXPERIMENTAL SECTION

Materials. All chemicals were purchased from Sigma-Aldrich and used as received unless noted otherwise. Deionized water (DIW) with resistivity >15 MΩ·cm was obtained from Millipore Elix 3. 2-(Dimethylamino)ethyl methacrylate (DMAEMA) was passed through an inhibitor-removal column (Sigma-Aldrich) before any polymerization reactions. 11-(2-Bromo-2-methyl)propionyloxy undecyl trichlorosilane (eBMPUS) was purchased from Gelest. Silicon wafers (p-doped, orientation ⟨100⟩) were purchased from Silicon Valley Microelectronics.

Sample Preparation. *Polymer Brush Formation.* We prepared substrates grafted with PDMAEMA by utilizing surface-initiated atom transfer radical polymerization (SI-ATRP). Silicon wafers (12 mm × 40 mm) were exposed to ultraviolet/ozone treatment (UVO, Model 42, Jelight Co.) for 30 min before use. The silane initiator (11-(2-bromo-2-methyl)propionyloxy undecyl trichlorosilane, eBMPUS) was deposited on the silicon wafer by incubating in a solution (0.005% v/v of eBMPUS in hexanes) at room temperature for 48 h. The ATRP solution containing DMAEMA (4 mL, 23.7 mM), DIW (36.8 mL, 2.0442 M), and isopropanol (9.2 mL, 120.3 mM) was prepared in a 150 mL round-bottom flask. The solution was purged with argon gas for 10 min. The ligand 2,2′-bipyridine (0.1421 g, 0.9 mM) and the catalyst CuCl (0.03917 g, 0.4 mM) were added to the solution; the solution was mixed using a stir bar and was degassed by blowing argon gas for 15 min. The PDMAEMA grafts were obtained by placing the initiator-coated substrates in a 20 mL vial filled with the ATRP solution for 120 min at room temperature.

SI-ATRP formed poly(2-(methacryloyloxy)ethyl-trimethylammonium chloride) (PMETAC) brushes. The ATRP solution contained [METAC]/[CuCl]/[2,2′-bipyridine] = [60]:[1]:[2.3]. The METAC monomer (11.46 mL, 60.1 mM) was with DIW (3.9 mL, 0.2163 M) and IPA (14.6 mL, 0.1916 M). Polymerization was carried out at room temperature for 5 h. The resulting dry brush thickness was ∼80 nm measured at 100 °C. For the poly(sulfobetaine methacrylate) (PSBMA) brushes, the ATRP solution was prepared by dissolving the monomer at a molar ratio of [SBMA]/[CuBr]/[2,2′-bipyridine] = [25]:[1]:[2]; 3.02 g (0.01 M) into the mixed solvent of DIW (5 mL, 0.2778 M) and methanol (15 mL, 0.1962 M). The SI-ATRP was performed at 60 °C for 24 h. The resulting dry brush thickness was ∼90 nm measured at 100 °C.

Quaternization Gradient of PDMAEMA. The PDMAEMA brushes were quaternized on a silicon substrate (6 mm × 40 mm) in the gaseous phase. The PDMAEMA brushes were placed vertically in an empty 10 ml glass beaker (inner diameter 2.5 cm, height 2.8 cm). Fifty microliters of 3.2 M methyl iodide−ethanol solution was injected into the beaker. After the desired reaction time (*e.g.*, 120 s), the specimen was removed from the beaker, rinsed with methanol, and dried with nitrogen gas.

Betainization of PDMAEMA. For the gaseous-phase modification, 20 μL of 0.1 M 1,3-propanesultone (P-S) in ethanol was injected in an airtight glass tube, where the PDMAEMA brush or qPDMAEMA brush sample was located. The glass tube was heated at 60 °C for 30 min. Since the volume of the reagent solution is small, most of it vaporized rapidly. The concentration of P-S and the reaction time varied depending on the degree of betainization. After the reaction, the sample was incubated in 1 M NaCl aqueous solution for 20 min to remove any electrostatically adsorbed counterions. Finally, the sample was rinsed with DIW followed by drying under a nitrogen gas flow. Seven milliliters of 0.1 M P-S solution in ethanol was utilized to immerse the entire sample substrate in the reagent solution for the liquid-phase modification. The remaining procedures were identical.

Bacterial Culture and Growth Conditions. *Escherichia coli* (*E. coli*) DH52 was obtained from the American Type Culture Collection (ATCC). For the bacterial experiments, bacterial cultures were grown on Luria-Bertani (LB) agar overnight at 37 °C. Bacterial cells were collected from the culture via an inoculation loop and suspended in LB broths. The optical density at 600 nm (OD_{600}) of the bacterial suspensions was then adjusted to 0.3. The substrate was submerged in 3 mL of a bacterial suspension in 24-well plates. The substrate was incubated at 25 °C in dark conditions and for 3 h.

Characterization. *Ellipsometry Measurements.* We utilized variable-angle spectroscopic ellipsometry (VASE) (J.A. Woollam Co.) to measure the thin film thickness and refractive index of the polymer. All samples were characterized by VASE at 100 °C with two angles of incidence (60 and 65° relative to the normal) and the wavelength ranging from 400 to 800 nm.[34] A hot stage (FP82HT, Mettler Toledo) connected to a central processor (FP90, Mettler Toledo) was placed on the VASE sample stage to carry out the high-temperature ellipsometry measurements. We analyzed the ellipsometry data with WVASE32 software (J.A. Woollam Co.). A single Cauchy layer model for polymers ($n = A_n + B_n/\lambda^2$), where n is the refractive index and A_n (=1.46−1.53) and B_n (=0.005−0.009 μm^2) are the fitting parameters on top of a 1.5 nm SiO_x layer and Si substrate was used to fit the experimental data.

FTIR Measurements. Fourier-transform infrared spectroscopy (FTIR) data were collected by performing 128 scans with a 4 cm^{-1} resolution in an attenuated total reflection (ATR) mode with Ge crystal on a Nicolet 6700 spectrometer and analyzed using OMNIC software. All spectra have been processed by advanced ATR correction followed by baseline correction.

Confocal Laser Scanning Microscopy Measurements and Data Analysis. Confocal laser scanning microscopy (CLSM) was performed on a Leica SP8 inverted microscope. The washed biofilms were fluorescently stained with a Viability/Cytotoxicity Assay Kit for Bacteria Live and Dead Cells (Biotum, CA). The kit includes DMAO and ethidium homodimer III (EthD-III). DMAO is a green-fluorescent nucleic acid dye that stains both live and dead bacteria. EthD-III is a red-fluorescent dye that selectively stains the dead cells with damaged cell membranes. Image J was employed to extract the green and red images from the raw CLSM files. These image files were further analyzed using CellC Cell Counting software.[35] Comparing the numbers of green (live) and red (dead) cells gives an estimate of cell viability on the investigated substrates.

■ RESULTS AND DISCUSSION

We studied the betainization of PDMAEMA brushes in the liquid and vapor phases.[24] In ethanol solution, P-S hydrolyzes, and the resulting sulfonic acid may protonate the repeat units of PDMAEMA and generate quaternary ammonium. The quaternary ammonium may, in turn, form ionic complexes with sulfonate groups in 3-ethoxypropanesulfonate, as shown in Figure 1. Therefore, we used betainization in the gaseous phase, using the procedures described in the Experimental Section.[31,32] This approach avoids hydrolyzation of P-S.

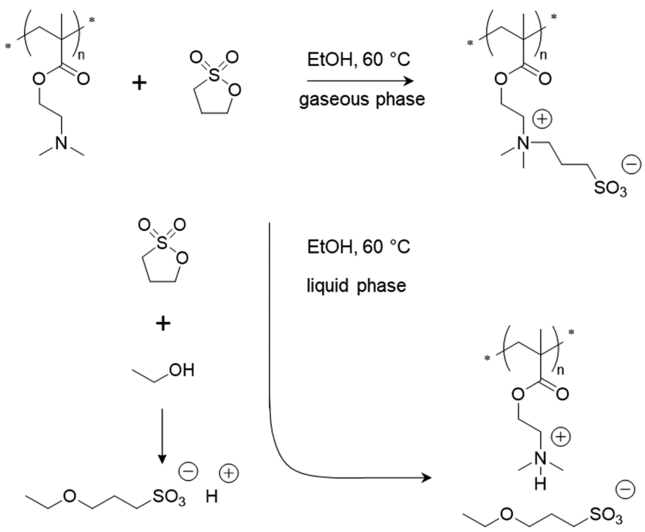

Figure 1. Reaction of PDMAEMA with 1,3-propanesultone in ethanol at 60 °C. In the liquid-phase reaction, the main products are the protonated PDMAEMA and 3-ethoxypropanesulfonate (undesired). In the gaseous-phase reaction, the main product is the betainized PDMAEMA (desired).

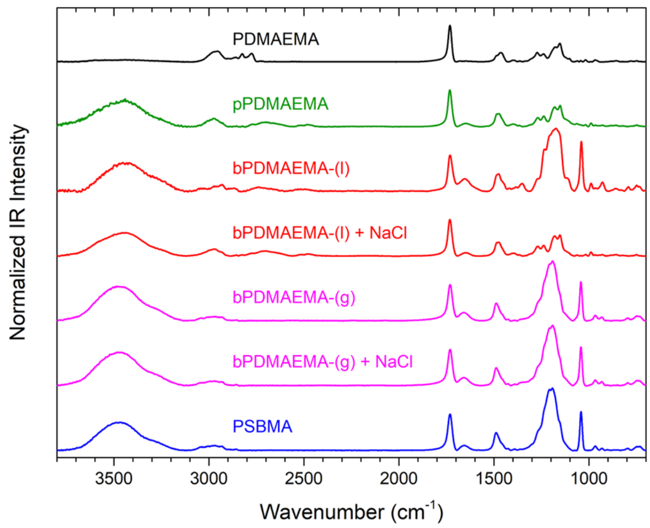

Figure 2. FTIR-ATR spectra (normalized to the carbonyl vibration at ~1731 cm^{-1}) collected from PDMAEMA,PSBMA, protonated PDMAEMA (pPDMAEMA), PDMAEMA betainized in the liquid phase (PDMAEMA (l)), and vapor phase (PDMAEMA-(g)). PDMAEMA-(l) + NaCl and PDMAEMA-(g) + NaCl are spectra collected from PDMAEMA-(l) and PDMAEMA-(g) after incubation in NaCl solution.

We carried out FTIR experiments to follow betainization in both liquid and vapor phases. Figure 2 plots FTIR-ATR spectra for PDMAEMA brushes after different treatments. When the PDMAEMA brushes get protonated (pPDMAEMA), broad O−H stretching bands appear at ~3300−3700 cm^{-1}, primarily due to water absorption. Also, the C−H stretching bands at ~2775 and ~2825 cm^{-1} disappear, and we observe two small broad bands at ~2481 and ~2701 cm^{-1} compared to the parent PDMAEMA. After betainization in the liquid phase (PDMAEMA (l)), two bands appear in the spectrum at ~1191 and ~1042 cm^{-1}, corresponding to S═O stretching and SO_3^- stretching, respectively. The modified brushes were incubated in 1 M of NaCl solution for 20 min to remove any residual ionic complexes from the sample surfaces. The FTIR spectrum from a sample after betainization in the liquid phase and subsequent incubation in NaCl (PDMAEMA (l) + NaCl) does not contain the sulfonate bands (~1191 and ~1042 cm^{-1}); the PDMAEMA (l) + NaCl spectrum is identical to that of pPDMAEMA, implying betainization did not occur. FTIR spectrum collected from a sample that was betainized in the vapor phase (PDMAEMA (g)) does not change even after incubation in NaCl (PDMAEMA (g) + NaCl). Both spectra match that collected from poly(sulfobetaine methacrylate) (PSBMA) brushes.

Figure 3 displays the experimental procedure for fabricating the counterpropagating gradients (CPGs) of quaternized and betainized polymer brushes. We prepared PDMAEMA brushes (~95 nm, dry thickness measured at 100 °C) having comparable grafting density (assuming ~0.5 chains/nm^2) and molecular weight (~150.8 kDa) from surface-initiated atom transfer radical polymerization (SI-ATRP).[36−38] We gradually modified the PDMAEMA grafts spatially to various degrees of quaternization (DQ) by following the methodology outlined in our previous work.[17] The gaseous-phase quaternization involves four processes: (i) evaporation of the quaternizing reagent (*i.e.*, MI), (ii) diffusion of MI through the air, (iii) diffusion of MI through the polymer film, and (iv) the reaction of MI with the polymer. The diffusion through the air is the rate-limiting step.[17] The resulting surface features a number density gradient in the quaternized units. One can adjust gradient properties (*i.e.*, width and amplitude) by changing the MI solution concentration, the processing time, and the shape and size of the glass container for MI solution.

In the subsequent step, we placed the quaternized specimens vertically in a glass reactor with 20 μL of ethanol solution dissolving P-S at 60 °C (closed-cap). P-S only reacts with the remaining tertiary amines in PDMAEMA but not the quaternary ammonium in qPDMAEMA (*cf.* Figure S1). The degree of modification can be controlled by the reaction time and P-S concentration (*cf.* Figure S2).

The resulting CPG sample was analyzed spatially with FTIR-ATR (*cf.* Figure 4). After baseline subtraction, every spectrum was normalized by the intensity at ~1731 cm^{-1} (the carbonyl group in the repeat units), which should remain unaffected by quaternization and betainization. Two distinct vibration bands, at ~956 and ~1042 cm^{-1} (blue and red bands in Figure 4a), were selected to determine the degree of quaternization (DQ) and degree of betainization (DB), respectively.[17,39] To obtain the saturated intensities of both bands, 100 mol % quaternized and betainized brushes (PMETAC and PSBMA) were synthesized directly using SI-ATRP of the corresponding monomers. The normalized intensities at ~956 and ~1042 cm^{-1} were measured for various positions in the CPG sample. The DQ and DB values were determined using eqs 1 and 2

https://doi.org/10.1021/acs.biomac.1c01386
Biomacromolecules 2022, 23, 424−430

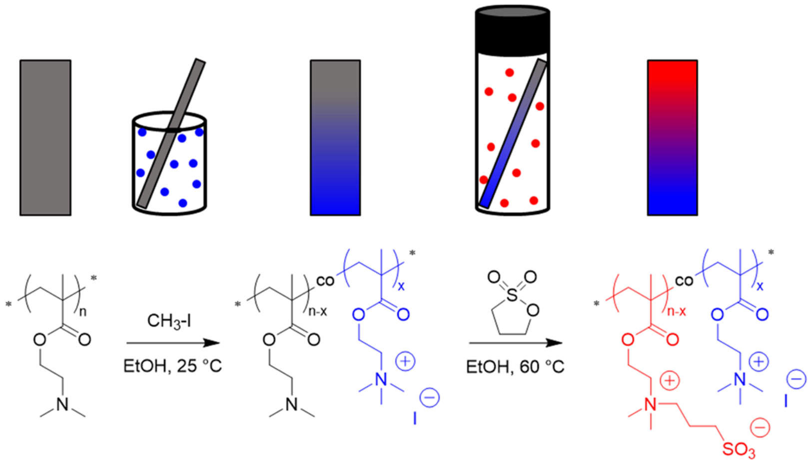

Figure 3. Postpolymerization modification processes for fabricating the counterpropagating gradients (CPGs) of quaternized and betainized PDMAEMA brushes. Both quaternization and betainization are carried out in the gaseous phase.

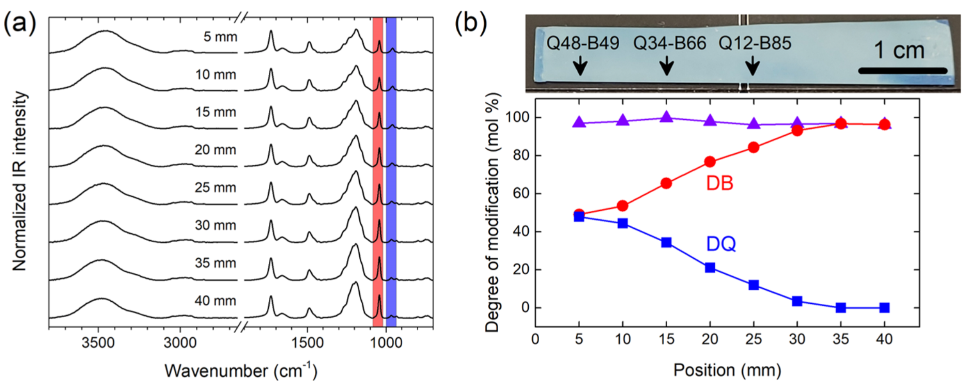

Figure 4. (a) FTIR-ATR spectra (normalized to the carbonyl vibration at ∼1731 cm^{-1}) collected at different locations on the counterpropagating gradients of quaternized and betainized PDMAEMA brushes. The number above each spectrum denotes the distances from the "quaternized edge" of the sample. The bands at ∼1042 cm^{-1} (red) and ∼956 cm^{-1} (blue) represent the relative variation of the degree of betainization (DB) and degree of quaternization (DQ), respectively. (b) DQ (blue squares), DB (red circles), and total (purple up-triangles) at various positions in the sample (measured from the quaternized edge of the sample). The scale bar corresponds to 1 cm.

$$\mathrm{DQ}\,(\mathrm{mol}\,\%) = 100 \times \left[\frac{I_{\mathrm{sample}} - I_{\mathrm{PDMAEMA}}}{I_{\mathrm{PMETAC}} - I_{\mathrm{PDMAEMA}}}\right]_{956\ \mathrm{cm}^{-1}} \quad (1)$$

$$\mathrm{DB}\,(\mathrm{mol}\,\%) = 100 \times \left[\frac{I_{\mathrm{sample}} - I_{\mathrm{PDMAEMA}}}{I_{\mathrm{PSBMA}} - I_{\mathrm{PDMAEMA}}}\right]_{1042\ \mathrm{cm}^{-1}} \quad (2)$$

In eqs 1 and 2, I_{PDMAEMA}, I_{PMETAC}, and I_{PSBMA} indicate the normalized intensity of PDMAEMA, PMETAC, and PSBMA at the corresponding wavenumbers. As demonstrated by the data in Figure 4, profiles of DQ and DB in the sample display a counterpropagating character. The summation of the DQ and DB is ∼100 mol %, implying that nearly all tertiary amines in the polymer repeat units became modified. Our previous work reported a maximum DQ of ∼85%, attributed to the polymer steric hindrance due to limited solubility. The complete modification of all tertiary amines in PDMAEMA after quaternization and betainization reactions may be due to a higher solubility of sulfobetaine in ethanol relative to that of quaternary ammonium. The DQ and total concentration obtained from FTIR can be verified by ellipsometry (*cf.* Figure S3).[17]

We confirm the complete betainization of PDMAEMA by exposing PDMAEMA brushes to P-S in ethanol at 60 °C for various reaction times (*cf.* Figure S2). We used two P-S/ethanol solution concentrations: 0.01 and 0.1 M. In both instances, full betainization was achieved in less than ∼30 min, which is very fast compared to reactions carried out in the liquid phase (usually 6−48 h).[15,31,32,40−43] We attribute the rapid kinetics of reactants to (i) higher collision frequency and (ii) little ionic complexation in the gaseous phase relative to that in the solution phase.

The past few decades witnessed the development of several different types of antibacterial coatings. One of them involves quaternary amines with different lengths of the alkyl chain lengths.[44] A common problem with the antibacterial surface is that the dead bacterial cells remain attached to the surface after killing. Besides other complications, these cells block the active sites on the surface, which, in turn, loses its effectiveness. One way to address this issue is to make the coatings antifouling or remove the dead cells from the surface.[42,45−47] Here, we use the CPG surface to provide antibacterial and antifouling functions simultaneously. The surfaces of interest are at positions 5, 15, 25, and 35 mm from the quaternized edge of the sample. The [DQ,DB] values at those positions are [48,49], [34,66], [12,85], and [0,97] and they are denoted Q48−B49, Q34−B66, Q12−B85, and Q0−B97, respectively.

The CPG substrates were immersed in the suspension of *E. coli* and incubated for ∼3 h at 25 °C. After staining with a

https://doi.org/10.1021/acs.biomac.1c01386
Biomacromolecules 2022, 23, 424−430

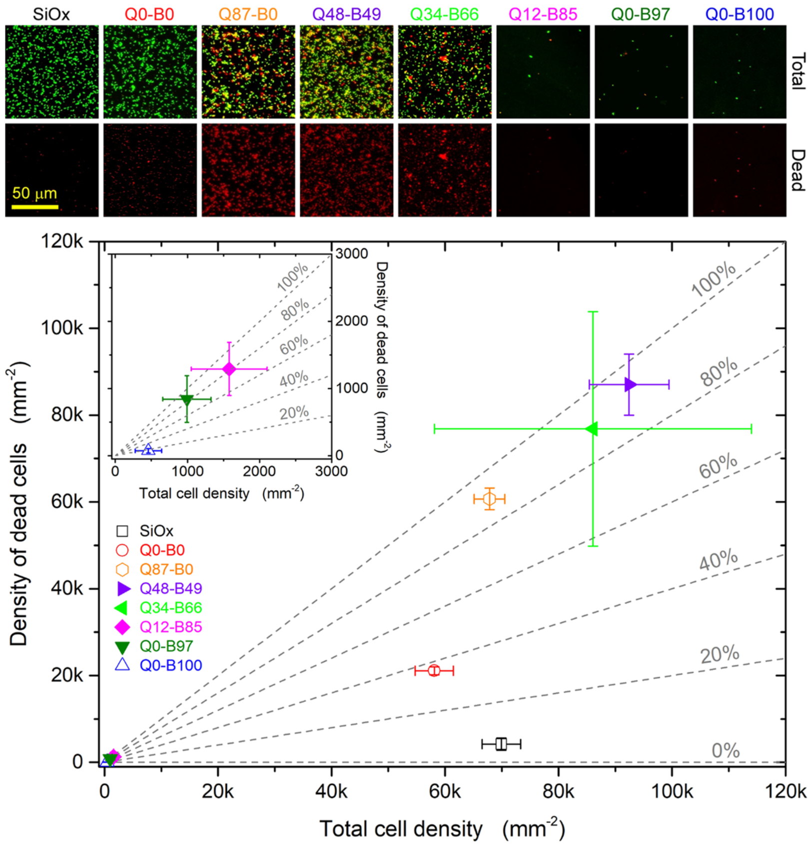

Figure 5. (Top) Confocal microscopy images of total cells and dead *E. coli* bacteria. The legend denotes the percentage of DQ and DB values. For example, Q48−B49 corresponds to 48 and 49 mol % of DQ and DB at the position, respectively. Live and dead *E. coli* cells are shown in green and red colors, respectively. The scanning area is ∼100 × 100 μm^2. (Bottom) The density of dead *E. coli* cells as a function of the total adsorbed *E. coli* cells.

Viability/Cytotoxicity Assay Kit for Bacteria Live and Dead Cells, the samples were imaged with CLSM and analyzed with CellC software. The dead cells appear red in the images, and the live cells display green in Figure 5. SiO_x and PDMAEMA (Q0−B0) brushes exhibit comparable total cell density without a noticeable bactericidal effect. Quaternized polymer brushes (Q87−B0) are antibacterial; they kill ∼90% of bacteria. Betainized brushes (Q0−B97, Q0−B100) exhibit antifouling behavior. The region Q48−B49 exhibits mainly antibacterial function with killing above ∼90% of bacteria. In the region Q34−B66, only ∼34 mol % of quaternary ammonium with methyl group killed ∼90% of bacteria on the surface. Also, the total cell density decreased slightly with increasing the degree of betainization. In regions Q12−B85 and Q0−B97, the trend changes dramatically. The surface predominantly shows antifouling function; only a few cells can be observed in the images. Despite the limited data set, it is safe to conclude that surfaces between Q34−B66 and Q12−B85 exhibit the dual functionality of antibacterial and antifouling functions concurrently.

In summary, we documented that betainization of PDMAEMA brushes using P-S proceeds more efficiently when carried out in the vapor phase (*i.e.*, evaporation of reagent solutions at 60 °C) than in the liquid phase. When reacting in the vapor phase, P-S does not form ionic complexes with PDMAEMA. The betainization reaction (pseudo-first-order in P-S), conducted with P-S ethanolic solutions with 0.01 and 0.1 M concentrations, resulted in complete betainization of PDMAEMA in <30 min. We generated counterpropagating gradients (CPGs) on PDMAEMA brushes by sequential and directional quaternization and betainization from the vapor phase. We established the degrees of quaternization (DQ) and betainization (DB) as a function of position on the sample using FTIR-ATR. We further employed CPG substrates in studying antibacterial and antifouling behaviors. While fully betainized samples exhibited antifouling behavior, specimens containing 12% of quaternized and 85% of betainized units acted simultaneously as antibacterial and antifouling surfaces.

■ ASSOCIATED CONTENT

Supporting Information

The Supporting Information is available free of charge at https://pubs.acs.org/doi/10.1021/acs.biomac.1c01386.

Ionic complexation between quaternary ammonium and sulfonate groups; reaction kinetics of PDMAEMA betainization from the vapor phase; quaternized and betainized counterpropagating gradients; and the density of dead and live *E. coli* cells on the substrate (PDF)

■ AUTHOR INFORMATION

Corresponding Author

Jan Genzer − *Department of Chemical and Biomolecular Engineering, North Carolina State University, Raleigh, North Carolina 27695-7905, United States; Global Station for Soft Matter, Global Institution for Collaborative Research and Education (GI-CoRE), Hokkaido University, Hokkaido 060-*

https://doi.org/10.1021/acs.biomac.1c01386
Biomacromolecules 2022, 23, 424−430

0808, Japan; orcid.org/0000-0002-1633-238X;
Email: jgenzer@ncsu.edu

Authors

Yeongun Ko − *Department of Chemical and Biomolecular Engineering, North Carolina State University, Raleigh, North Carolina 27695-7905, United States;* Present Address: Department of Chemical Engineering, University of Michigan, Ann Arbor, Michigan 48109-2800, United States; orcid.org/0000-0001-5770-6707

Vi Khanh Truong − *Department of Chemical and Biomolecular Engineering, North Carolina State University, Raleigh, North Carolina 27695-7905, United States; Nanobiotechnology Laboratory, School of Science, RMIT University, Melbourne, VIC 3000, Australia;* orcid.org/0000-0002-6016-6438

Sun Young Woo − *Department of Chemical and Biomolecular Engineering, North Carolina State University, Raleigh, North Carolina 27695-7905, United States*

Michael D. Dickey − *Department of Chemical and Biomolecular Engineering, North Carolina State University, Raleigh, North Carolina 27695-7905, United States;* orcid.org/0000-0003-1251-1871

Lilian Hsiao − *Department of Chemical and Biomolecular Engineering, North Carolina State University, Raleigh, North Carolina 27695-7905, United States;* orcid.org/0000-0002-4448-7397

Complete contact information is available at:
https://pubs.acs.org/10.1021/acs.biomac.1c01386

Notes

The authors declare no competing financial interest.

■ ACKNOWLEDGMENTS

This work was supported by the National Science Foundation, Grant no. DMR-1404639. The authors appreciate the partial support from the National Science Foundation, Grant no. DMR-1809453. Australian-American Fulbright Commission supported V.K.T.

■ REFERENCES

(1) Bhat, R. R.; Tomlinson, M. R.; Wu, T.; Genzer, J. Surface-Grafted Polymer Gradients: Formation, Characterization, and Applications. *Adv. Polym. Sci.* **2006**, *198*, 51−124.

(2) Genzer, J.; Bhat, R. R. Surface-Bound Soft Matter Gradients. *Langmuir* **2008**, *24*, 2294−2317.

(3) Genzer, J. Surface-Bound Gradients for Studies of Soft Materials Behavior. *Annu. Rev. Mater. Res.* **2012**, *42*, 435−468.

(4) Schreiber, F. Structure and Growth of Self-Assembling Monolayers. *Prog. Surf. Sci.* **2000**, *65*, 151−257.

(5) Pujari, S. P.; Scheres, L.; Marcelis, A. T. M.; Zuilhof, H. Covalent Surface Modification of Oxide Surfaces. *Angew. Chem., Int. Ed.* **2014**, *53*, 6322−6356.

(6) Chen, W. L.; Cordero, R.; Tran, H.; Ober, C. K. 50th Anniversary Perspective: Polymer Brushes: Novel Surfaces for Future Materials. *Macromolecules* **2017**, *50*, 4089−4113.

(7) Zoppe, J. O.; Ataman, N. C.; Mocny, P.; Wang, J.; Moraes, J.; Klok, H. A. Surface-Initiated Controlled Radical Polymerization: State-of-the-Art, Opportunities, and Challenges in Surface and Interface Engineering with Polymer Brushes. *Chem. Rev.* **2017**, *117*, 1105−1318.

(8) Pyun, J.; Kowalewski, T.; Matyjaszewski, K. Synthesis of Polymer Brushes Using Atom Transfer Radical Polymerization. *Macromol. Rapid Commun.* **2003**, *24*, 1043−1059.

(9) Divandari, M.; Trachsel, L.; Yan, W.; Rosenboom, J.-G.; Spencer, N. D.; Zenobi-Wong, M.; Morgese, G.; Ramakrishna, S. N.; Benetti, E. M. Surface Density Variation within Cyclic Polymer Brushes Reveals Topology Effects on Their Nanotribological and Biopassive Properties. *ACS Macro Lett.* **2018**, *7*, 1455−1460.

(10) Divandari, M.; Morgese, G.; Trachsel, L.; Romio, M.; Dehghani, E. S.; Rosenboom, J.-G.; Paradisi, C.; Zenobi-Wong, M.; Ramakrishna, S. N.; Benetti, E. M. Topology Effects on the Structural and Physicochemical Properties of Polymer Brushes. *Macromolecules* **2017**, *50*, 7760−7769.

(11) Galvin, C. J.; Genzer, J. Applications of Surface-Grafted Macromolecules Derived from Post-Polymerization Modification Reactions. *Prog. Polym. Sci.* **2012**, *37*, 871−906.

(12) Günay, K. A.; Theato, P.; Klok, H.-A. Standing on the Shoulders of Hermann Staudinger: Post-Polymerization Modification from Past to Present. *J. Polym. Sci., Part A: Polym. Chem.* **2013**, *51*, 1−28.

(13) Das, A.; Theato, P. Activated Ester Containing Polymers: Opportunities and Challenges for the Design of Functional Macromolecules. *Chem. Rev.* **2016**, *116*, 1434−1495.

(14) Gauthier, M. A.; Gibson, M. I.; Klok, H.-A. Synthesis of Functional Polymers by Post-Polymerization Modification. *Angew. Chem., Int. Ed.* **2009**, *48*, 48−58.

(15) Song, L.; Lam, Y. M. Selective Betainization of PS−P4VP and Solution Properties. *Langmuir* **2006**, *22*, 319−324.

(16) Jhon, Y. K.; Semler, J. J.; Genzer, J. Effect of Solvent Quality and Chain Confinement on the Kinetics of Polystyrene Bromination. *Macromolecules* **2008**, *41*, 6719−6727.

(17) Ko, Y.; Christau, S.; Von Klitzing, R.; Genzer, J. Charge Density Gradients of Polymer Thin Film by Gaseous Phase Quaternization. *ACS Macro Lett.* **2020**, *9*, 158−162.

(18) Barbey, R.; Laporte, V.; Alnabulsi, S.; Klok, H.-A. Postpolymerization Modification of Poly(Glycidyl Methacrylate) Brushes: An XPS Depth-Profiling Study. *Macromolecules* **2013**, *46*, 6151−6158.

(19) Arifuzzaman, S.; Özçam, A. E.; Efimenko, K.; Fischer, D. A.; Genzer, J. Formation of Surface-Grafted Polymeric Amphiphilic Coatings Comprising Ethylene Glycol and Fluorinated Groups and Their Response to Protein Adsorption. *Biointerphases* **2009**, *4*, FA33−FA44.

(20) Pandiyarajan, C. K.; Rubinstein, M.; Genzer, J. Surface-Anchored Poly(N-Isopropylacrylamide) Orthogonal Gradient Networks. *Macromolecules* **2016**, *49*, 5076−5083.

(21) Pandiyarajan, C. K.; Genzer, J. Thermally Activated One-Pot, Simultaneous Radical and Condensation Reactions Generate Surface-Anchored Network Layers from Common Polymers. *Macromolecules* **2019**, *52*, 700−707.

(22) Pandiyarajan, C. K.; Genzer, J. UV- and Thermally-Active Bifunctional Gelators Create Surface-Anchored Polymer Networks. *Macromol. Rapid Commun.* **2021**, *42*, No. 2100266.

(23) Paschke, S.; Lienkamp, K. Polyzwitterions: From Surface Properties and Bioactivity Profiles to Biomedical Applications. *ACS Appl. Polym. Mater.* **2020**, *2*, 129−151.

(24) Fischer, R. F. Propanesultone. *Ind. Eng. Chem.* **1964**, *56*, 41−45.

(25) Rawlinson, L.-A. B.; Ryan, S. M.; Mantovani, G.; Syrett, J. A.; Haddleton, D. M.; Brayden, D. J. Antibacterial Effects of Poly(2-(Dimethylamino Ethyl)Methacrylate) against Selected Gram-Positive and Gram-Negative Bacteria. *Biomacromolecules* **2010**, *11*, 443−453.

(26) Li, B.; Jain, P.; Ma, J.; Smith, J. K.; Yuan, Z.; Hung, H. C.; He, Y.; Lin, X.; Wu, K.; Pfaendtner, J.; Jiang, S. Trimethylamine N-Oxide−Derived Zwitterionic Polymers: A New Class of Ultralow Fouling Bioinspired Materials. *Sci. Adv.* **2021**, *5*, No. eaaw9562.

(27) Schlenoff, J. B. Zwitteration: Coating Surfaces with Zwitterionic Functionality to Reduce Nonspecific Adsorption. *Langmuir* **2014**, *30*, 9625−9636.

(28) Laschewsky, A.; Rosenhahn, A. Molecular Design of Zwitterionic Polymer Interfaces: Searching for the Difference. *Langmuir* **2019**, *35*, 1056−1071.

(29) Baggerman, J.; Smulders, M. M. J.; Zuilhof, H. Romantic Surfaces: A Systematic Overview of Stable, Biospecific, and Antifouling Zwitterionic Surfaces. *Langmuir* **2019**, *35*, 1072−1084.
(30) Jiang, S.; Ishihara, K.; Iwasaki, Y.; Vancso, J. Zwitterionic Interfaces: Concepts and Emerging Applications Special Issue. *Langmuir* **2019**, *35*, 1055.
(31) Yang, R.; Xu, J.; Ozaydin-Ince, G.; Wong, S. Y.; Gleason, K. K. Surface-Tethered Zwitterionic Ultrathin Antifouling Coatings on Reverse Osmosis Membranes by Initiated Chemical Vapor Deposition. *Chem. Mater.* **2011**, *23*, 1263−1272.
(32) Yang, R.; Gleason, K. K. Ultrathin Antifouling Coatings with Stable Surface Zwitterionic Functionality by Initiated Chemical Vapor Deposition (ICVD). *Langmuir* **2012**, *28*, 12266−12274.
(33) Hart, R.; Timmerman, D. New Polyampholytes: The Polysulfobetaines. *J. Polym. Sci.* **1958**, *28*, 638−640.
(34) Ko, Y.; Miles, J. R.; Genzer, J. Determining Water Sorption and Desorption in Thin Hydrophilic Polymer Films by Thermal Treatment. *ACS Appl. Polym. Mater.* **2019**, *1*, 2495−2502.
(35) Selinummi, J.; Seppälä, J.; Yli-Harja, O.; Puhakka, J. A. Software for Quantification of Labeled Bacteria from Digital Microscope Images by Automated Image Analysis. *Biotechniques* **2005**, *39*, 859−863.
(36) Patil, R. R.; Turgman-Cohen, S.; Šrogl, J.; Kiserow, D.; Genzer, J. On-Demand Degrafting and the Study of Molecular Weight and Grafting Density of Poly(Methyl Methacrylate) Brushes on Flat Silica Substrates. *Langmuir* **2015**, *31*, 2372−2381.
(37) Patil, R. R.; Turgman-Cohen, S.; Šrogl, J.; Kiserow, D.; Genzer, J. Direct Measurement of Molecular Weight and Grafting Density by Controlled and Quantitative Degrafting of Surface-Anchored Poly(Methyl Methacrylate). *ACS Macro Lett.* **2015**, *4*, 251−254.
(38) Ko, Y.; Miles, J. R.; Genzer, J. Determining Water Sorption and Desorption in Thin Hydrophilic Polymer Films by Thermal Treatment. *ACS Appl. Polym. Mater.* **2019**, *1*, 2495−2502.
(39) Walker, E. J.; Pandiyarajan, C. K.; Efimenko, K.; Genzer, J. Generating Surface-Anchored Zwitterionic Networks and Studying Their Resistance to Bovine Serum Albumin Adsorption. *ACS Appl. Polym. Mater.* **2019**, *1*, 3323−3333.
(40) Bütün, V. Selective Betainization of 2-(Dimethylamino)Ethyl Methacrylate Residues in Tertiary Amine Methacrylate Diblock Copolymers and Their Aqueous Solution Properties. *Polymer* **2003**, *44*, 7321−7334.
(41) Pei, Y.; Lowe, A. B. Polymerization-Induced Self-Assembly: Ethanolic RAFT Dispersion Polymerization of 2-Phenylethyl Methacrylate. *Polym. Chem.* **2014**, *5*, 2342−2351.
(42) Widyaya, V. T.; Müller, C.; Al-Ahmad, A.; Lienkamp, K. Three-Dimensional, Bifunctional Microstructured Polymer Hydrogels Made from Polyzwitterions and Antimicrobial Polymers. *Langmuir* **2019**, *35*, 1211−1226.
(43) Zhang, C.; Yin, C.; Wang, Y.; Zhou, J.; Wang, Y. Simultaneous Zwitterionization and Selective Swelling-Induced Pore Generation of Block Copolymers for Antifouling Ultrafiltration Membranes. *J. Membr. Sci.* **2020**, *599*, No. 117833.
(44) Koufakis, E.; Manouras, T.; Anastasiadis, S. H.; Vamvakaki, M. Film Properties and Antimicrobial Efficacy of Quaternized PDMAEMA Brushes: Short vs Long Alkyl Chain Length. *Langmuir* **2020**, *36*, 3482−3493.
(45) Lv, J.; Jin, J.; Chen, J.; Cai, B.; Jiang, W. Antifouling and Antibacterial Properties Constructed by Quaternary Ammonium and Benzyl Ester Derived from Lysine Methacrylamide. *ACS Appl. Mater. Interfaces* **2019**, *11*, 25556−25568.
(46) Liu, T.; Yan, S.; Zhou, R.; Zhang, X.; Yang, H.; Yan, Q.; Yang, R.; Luan, S. Self-Adaptive Antibacterial Coating for Universal Polymeric Substrates Based on a Micrometer-Scale Hierarchical Polymer Brush System. *ACS Appl. Mater. Interfaces* **2020**, *12*, 42576−42585.
(47) Zou, Y.; Zhang, Y.; Yu, Q.; Chen, H. Dual-Function Antibacterial Surfaces to Resist and Kill Bacteria: Painting a Picture with Two Brushes Simultaneously. *J. Mater. Sci. Technol.* **2021**, *70*, 24−38.

https://doi.org/10.1021/acs.biomac.1c01386
Biomacromolecules 2022, 23, 424−430